Acta metall. Vol. 36, No. 4, pp. 1043–1051, 1988
Printed in Great Britain.

0001-6160/88 $3.00+0.00

THE KINETICS OF DISLOCATION CLIMB OVER HARD PARTICLES—I. CLIMB WITHOUT ATTRACTIVE PARTICLE–DISLOCATION INTERACTION

J. RÖSLER and E. ARZT
Max-Planck-Institut für Metallforschung, Seestraße 92, D-7000 Stuttgart 1, F.R.G.

(*Received* 18 *May* 1987)

Abstract—The effect of hard particles of low volume fraction on the creep strength is studied theoretically in a two-part paper. Here in part I, the kinetics of dislocation climb over a particle is modelled assuming that the particle does not exert an attractive force on the dislocation ("non-interacting" particle). The shape of the climbing dislocation is given by a minimum energy condition, which is shown to rule out purely "local" climb (as considered in previous models). A natural power-law dependence of the dislocation velocity on the applied stress, with n ranging from about 3 to 4, is obtained, and only a small threshold stress can be identified. The results appear compatible with the creep behaviour of alloys strengthened by coherent precipitates, but are totally at variance with experimental threshold stress data for materials with incoherent particle dispersions.

Résumé—Nous présentons dans un article en deux parties une étude théorique de l'effet des particules dures de faible fraction volumique sur la résistance au fluage. Dans cette première partie, nous modélisons la cinétique de la montée d'une dislocation qui franchit une particule en supposant que la particule n'attire pas la dislocation (particule non interactive). La forme de la dislocation qui monte est donnée par une condition d'énergie minimale qui exclut la montée purement "locale" que l'on considérait dans les modèles précédents. Nous trouvons que la vitesse des dislocations varie en fonction de la contrainte appliquée selon une loi de puissance naturelle, avec n variant d'environ 3 à 4; nous n'avons pu identifier qu'une faible contrainte-seuil. Les résultats semblent compatibles avec le comportement en fluage des alliages durcis par des précipités cohérents, mais ils sont en désaccord complet avec les résultats expérimentaux concernant le seuil de contrainte dans les matériaux comportant des dispersions de particules incohérentes.

Zusammenfassung—Der Einfluß harter Teilchen in geringem Volumanteil auf das Kriechen wird in einer zweiteiligen Arbeit theoretisch behandelt. In diesem ersten Teil wird die Kinetik des Kletterns von Versetzungen über ein Teilchen betrachtet. Im Modell wird angenommen, daß das Teilchen keine attraktive Wechselwirkung mit der Versetzung aufweist ('nicht-wechselwirkendes' Teilchen). Die Form der kletternden Versetzung wird durch eine Bedingung minimaler Energie bestimmt, welche -wie gezeigt wird- reines "lokales" Klettern (welches in früheren Modellen betrachtet worden ist) ausschließt. Es ergibt such eine natürliche Potenzgesetz-Abhängigkeit der Versetzungsgeschwindigkeit von der äußeren Spannung, wobei n zwischen 3 und 4 liegt; nur eine kleine Schwellspannung kann gefunden werden. Die Ergebnisse scheinen mit dem Kriechverhalten von Legierungen, die durch kohärente Ausscheidungen gehärtet sind, verträglich zu sein. Sie sind jedoch vollständig unverträglich mit experimentellen Ergebnissen über die Schwellspannung von Materialien mit Dispersionen inkohärenter Teilchen.

1. INTRODUCTION

The presence of hard particles can improve the mechanical behaviour of metallic materials at high temperature in different ways. Alloys which are strengthened by coherent precipitates, for example, exhibit higher creep resistance [1–3] than the particle-free matrix, provided the particle microstructure does not degrade too rapidly during the thermal exposure. Dispersion strengthened high temperature alloys exploit another, much more pronounced effect: the incoherent dispersoid particles introduce a clear threshold stress below which the rate of creep deformation is negligible and stress rupture lives become exceedingly large, e.g. [4–10].

How these technically important effects can be explained in terms of dislocation theory has been discussed in the literature over the past 15 years [9, 11–15], but the mechanisms are not as yet fully understood. There is general agreement that at high temperatures and relatively low stresses both non-shearable dispersoids and shearable precipitates are climbed over by lattice dislocations. It is this climb mechanism (rather than particle cutting or Orowan bowing, which predominate at higher stresses and/or lower temperatures) with which the present paper—part I here and part II [16]—is concerned.

Up to now, two kinds of models for dislocation climb over particles have been put forward:

—models based on the "local climb" assumption,

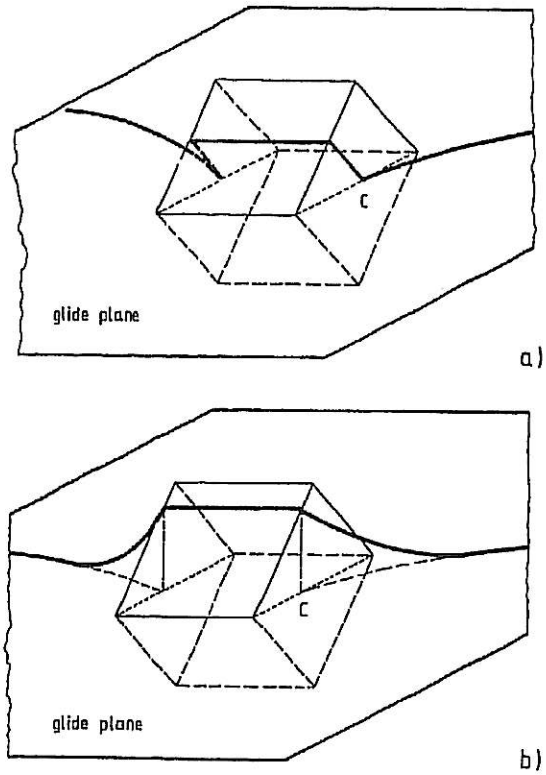

Fig. 1. Schematic profile of a dislocation climbing over a cube-shaped particle, according to different model assumptions: (a) "local" climb, with a sharp dislocation bend at C, and (b) "general" climb, where the high curvature at C is relaxed by "unravelling".

which postulate that the climbing dislocation segment profiles the dispersoid, and the dislocation between the dispersoids remains in its glide plane [11, 13] [Fig. 1(a)], and

—models based on "general climb", in which the dislocation is allowed to "unravel", i.e. to reduce, under the action of its line tension, the high curvature at the point where it meets the dispersoid [12, 14] [Fig. 1(b)].

Whether or not a threshold stress for dislocation climb is predicted by these models depends sensitively on which dislocation geometry has been postulated [15]. During "local" climb a significant amount of new dislocation line has to be created, leading to a threshold shear stress which depends on particle shape and is roughly given by [11, 13]

$$\tau_{th} \approx (0.4 \ldots 0.7)\tau_0 \qquad (1)$$

where τ_0 is the Orowan stress in shear [see equation (2) below]. Although this is a correct order-of-magnitude estimate for creep thresholds measured in dispersion strengthened materials, it can be argued rightly [12] that "local" climb is an extremely unstable process: the sharp bend in the dislocation, which is instrumental in producing a threshold stress, can be rapidly relaxed by diffusion, leading to more "general" climb. For "general" climb, however, only small [9, 14, 15] threshold stresses are predicted; depending on the particle statistics, it can lie about as low as $0.04\, f\tau_0$ (where f is the particle volume fraction). Therefore, while the exact dislocation shape which would be appropriate is still controversial, it is likely that the agreement of the "local" climb theory with threshold stress values for dispersion strengthened materials is fortuitous.

Besides the energetics of the climb process itself, an attractive particle–dislocation interaction has been suggested as another reason for the existence of a threshold stress [17–21]. This hypothesis is supported by TEM observations of dislocation structures in crept dispersion strengthened alloys [18, 20]. An attractive interaction may also localize climb; but since only the energetics of this attraction, with fixed dislocation geometry, has been considered so far, its effect on the climb kinetics is unknown. What is lacking therefore is (i) a kinetic analysis of dislocation climb over particles without arbitrary assumptions on dislocation shape, and (ii) a study of the effect of particle–dislocation attraction on this kinetics.

The present paper reports on part I of a theoretical study carried out with the aim to fill these gaps in the fundamental understanding of particle strengthening at high temperatures. We treat, to a good approximation, the full kinetics of dislocation climb over a "non-interacting" dispersoid particle of simple shape, under only one assumption concerning dislocation geometry: the climbing dislocation segment is required to have constant chemical potential for vacancies along its length (minimum energy assumption). Attractive interactions and their implications for the kinetics of climb are dealt with in part II [16].

2. THE STRUCTURE OF THE MODEL

The geometry of the model follows the earlier approaches by Brown and Ham [11] and Lagneborg [12]. Consider a dispersion of particles with low volume fraction f and mean planar spacing 2λ. The particles have rectangular cross section, with edge length d; their faces are inclined at an angle β to the slip plane of the dislocations [Fig. 2(a)]. It is assumed here in part I that except for the short-range repulsion, no attractive or long-range repulsive interaction between particles and dislocations exists; in this sense we will call the particles "non-interacting". The line energy of the dislocation is taken as constant over its entire length.

The shear stress necessary for particle by-pass by athermal dislocation bowing is given by the Orowan stress, which in its simplest form is

$$\tau_0 = \frac{Gb}{2\lambda} \qquad (2)$$

where G is the shear modulus of the material and b the magnitude of a lattice dislocation Burgers vector. Under the action of a shear stress below the Orowan stress, dislocations glide a short distance until they become pinned by the dispersoids. As the dislocation now climbs up on the particle to position z_0 (Fig. 2),

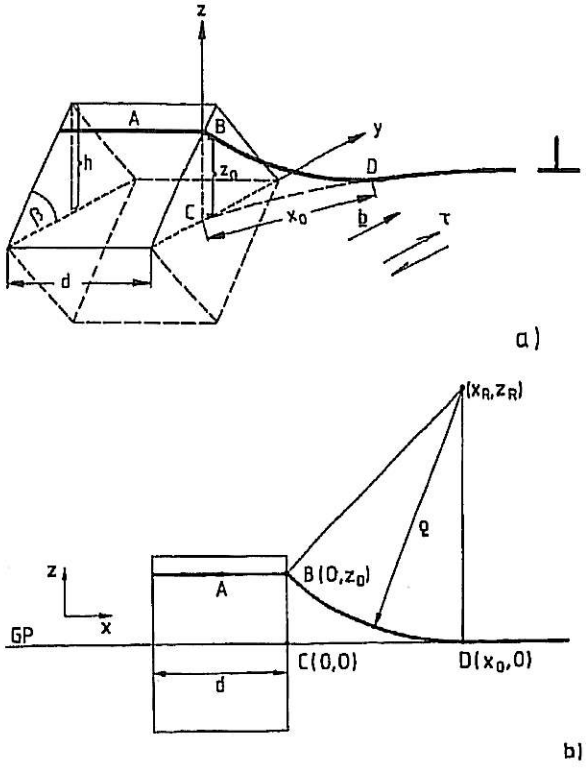

Fig. 2. Geometrical details referred to in the development of the present model: (a) perspective view, identifying particle height h, edge length d and ramp angle β, and the dislocation shape parameters x_0, z_0; (b) projected view after rolling out the cylindrical surface (BCD) onto the plane of the paper. The dislocation segment BD is assumed to be a circular arc in this projection. The x-axis runs along CD. GP = glide plane.

it leaves its glide plane, under the action of its line tension, up to an unspecified distance x_0 from the particle surface. The projected shape of such a dislocation is shown in Fig. 2(b): a straight horizontal line at the particle (A–B) which links up with a segment in the matrix (B–D). As in [12], the segment is assumed to have constant curvature when the cylindrical surface on which it lies is rolled out onto a plane—an assumption which simplifies an otherwise intractable analysis. Because the projected glide plane must be tangent to the circular segment at x_0, the dislocation position and shape are uniquely described by specifying z_0 and x_0.

In the present model the extent to which climb is localized at the particle will be determined by equilibrium: for a given z_0, the unravelling distance x_0 is fixed by the condition that the driving forces for vacancy absorption along AB (due to the applied stress) and along BD (due to dislocation curvature out of its glide plane) be identical; otherwise a short-range diffusive flux would rapidly establish this equilibrium. The driving force for dislocation climb is then given by the chemical potential μ_{ABD} along ABD; it will be calculated in Section 3.

In order to surmont a dispersoid by climb. a positive edge dislocation like the one shown in Fig. 2 absorbs vacancies which it receives by diffusion. Two diffusion paths are possible [13]: either pipe diffusion from the neighbouring particle (where on average the dislocation will be climbing in the opposite direction) or volume diffusion (from a source, defined to be at infinity, with a vacancy concentration corresponding to thermal equilibrium). The resulting forward velocity dy/dt of the dislocation is determined by the flux of vacancies arriving at segment A–D. Therefore dy/dt is derived from Fick's law, giving

$$\frac{dy}{dt}(x_0, z_0) = C_i \frac{|\mu_{ABD}(x_0, z_0)|}{|dA_{ABD}/dy\,(x_0, z_0)|} \tag{3}$$

A_{ABD} is the area under the climbing segment A–D, projected in the direction of the Burgers vector, such that (dA_{ABD}/dy) is proportional to the number of vacancies required for a unit advance of the dislocation. C_i is a kinetic constant which for volume diffusion control is approximately equal to [13]

$$C_v = \frac{2\pi D_v d}{k_B T b}. \tag{4}$$

If pipe diffusion from the neighbouring particle is rate-limiting then [13]

$$C_p = \frac{a_p D_p}{k_B T \lambda b} \tag{5}$$

D_v is the volume diffusitivity, D_p the pipe diffusivity, and $k_B T$ the thermal energy. The linearity in $|\mu|$ in equation (3) holds only for $|\mu| \ll k_B T$ which is satisfied for particles larger than a few nm.

Equation (3) expresses the trade-off between the kinetics and the energetics of the dislocation process: if climb is "general", i.e. x_0 is large, the additional line length and the resulting energy penalty are small, leading to large $|\mu|$, but the number of vacancies needed to support this long-range climb process (proportional to dA_{ABD}/dy) is also large, which slows down the rate. Conversely, if climb is nearly "local", much additional line energy has to be expended, but fewer vacancies are necessary; thus the process is fast, provided the applied stress is sufficiently high to allow enough new line length to be formed. This kinetic argument has been put forward by Shewfelt and Brown [13] to support the "local" climb hypothesis, but as will be shown, for energetic reasons climb is never truly local in the absence of an attractive particle–dislocation interaction.

3. THE EQUILIBRIUM DISLOCATION PROFILE

First we establish the chemical potentials for vacancies along the dislocation segments A–B and B–D, and then equate them to obtain the equilibrium value of x_0. Despite the simple particle shape, the mathematical treatment is complicated; the reader is referred to the Appendix and to [22] for details. The symbols used are listed in Table 1 of part II [16].

The driving force for adding vacancies to the dislocation segment AB is the work done by forward glide of the entire dislocation when it climbs higher at the particle. At the same time, extra dislocation line of infinitesimal length dl and specific energy T_{BD} has to be created along B–D. As a result, the chemical potential along A–B is (Appendix)

$$\mu_{AB} = \frac{2a_v}{d}\left[T_{BD}\left(\frac{\partial l}{\partial z_0}\right)_{A_{BD}} - \frac{\tau\lambda b}{\tan\beta}\right]. \tag{6}$$

Here $a_v \approx b^2$ is the cross sectional area of a vacancy and τ the applied shear stress. The line length differential is well approximated by

$$\left(\frac{\partial l}{\partial z_0}\right)_{A_{BD}} \cong 1 - \left(1 - \frac{z_0}{x_0}\right)^{9/4}. \tag{7}$$

Note that μ_{AB} becomes more positive with increasing z_0/x_0. Because z_0/x_0 always increases during climb, the driving force at AB diminishes as the dislocation climbs up the dispersoid.

Along BD, the driving force for adding a vacancy is the resulting reduction in dislocation curvature. Thus the chemical potential is (Appendix)

$$\mu_{BD} = -T_{BD}\, a_v \frac{1}{\rho}\frac{1}{\sqrt{1-(\tau/\tau_0)^2}} \tag{8}$$

where the radius of curvature ρ of the dislocation depends on x_0 and z_0

$$\rho = \frac{z_0}{2}\left[\left(\frac{x_0}{z_0}\right)^2 + 1\right]. \tag{9}$$

The square-root factor in equation (8) accounts approximately for the screw component of the edge dislocation in the vicinity of the dispersoid. We note that μ_{BD} is always negative, with its absolute value decreasing as the dislocation unravels.

The equilibrium shape $x_0(z_0)$ is obtained implicitly by equating μ_{AB} and μ_{BD}:

$$x_0 = d\left\{\sqrt{1-(\tau/\tau_0)^2}\left(\frac{x_0}{z_0}+\frac{z_0}{x_0}\right) \times\left[\frac{\tau}{\tau_0}\frac{1}{\tan\beta} - 1 + \left(1-\frac{z_0}{x_0}\right)^{9/4}\right]\right\}^{-1}. \tag{10}$$

This equation can be solved numerically. The results are shown in Fig. 3, with two dislocation profiles illustrated in Fig. 4.

By inserting the result in equation (6) [or equivalently in equation (8)], the equilibrium chemical potential along ABD is obtained. Also the increment of the area under the dislocation can now be expressed as a function of z_0 (see Appendix). The final solution for the dislocation velocity is obtained by inserting equation (6) (or 8), using equations (7) (or 9) and (10), and an expression for the area increment, in equation (3). Integration yields the time for a dis-

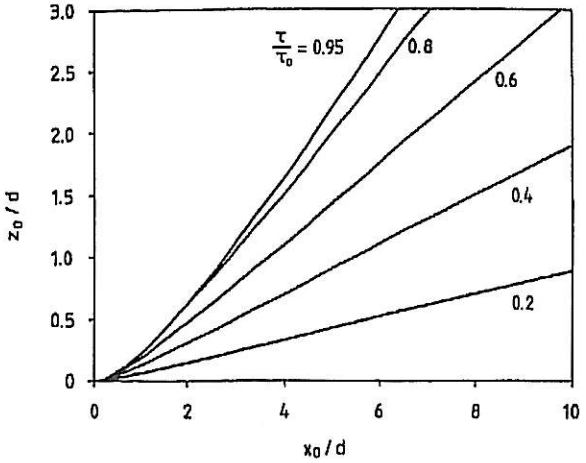

Fig. 3. The equilibrium unravelling distance x_0 as a function of z_0, both in units of the particle edge length d [equation (10)], for $\beta = 45°$. The parameter shown is the applied stress, in units of the Orowan stress. Note that truly local climb ($x_0 = 0$) is never stable.

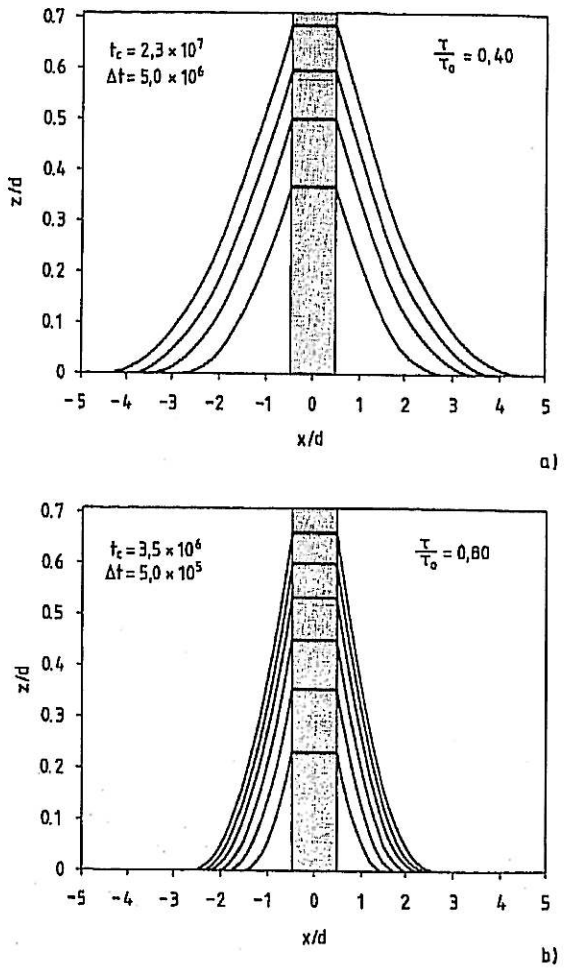

Fig. 4. Calculated dislocation profiles in the vicinity of a cube-shaped particle with ramp angle $\beta = 45°$, after equidistant time steps Δt [same projection as in Fig. 2(b)]. The particle (shaded) appears distorted as a result of different scaling of the axes. The abscissa coincides with the trace of the glide plane. (a) At an applied stress $\tau = 0.4\ \tau_O$, giving a by-pass time $t_c = 2.3 \times 10^7$ (arbitrary units), and (b) $\tau = 0.8\ \tau_O$, with a by-pass time $t_c = 3.5 \times 10^6$ (same units). Note increasing climb localization on increasing stress.

location to complete climb over a given particle

$$t_c = \int_{y_{min}}^{y_{max}} \frac{1}{\mathrm{d}y/\mathrm{d}t}\,\mathrm{d}y. \tag{11}$$

Results of these calculations, which can only be carried out numerically, are illustrated in Figs 7 and 8 and will be discussed in Section 5.

4. THRESHOLD STRESS DUE TO RESTRICTED CLIMB

The calculations described above apply strictly only for the case of infinite particle spacings (zero volume fraction), such that the unravelling process can occur up to arbitrarily large values of x_0. In a random array of particles with finite volume fraction, a dislocation will thread over and under neighbouring particles, which makes the midpoint between them a limit for x_0 (see Fig. 5). The maximum value of x_0 is given by

$$x_0^{max} = \frac{\lambda}{\tau/\tau_0}\cdot\arcsin\frac{\tau}{\tau_0}. \tag{12}$$

Further particle bypass occurs by a process which we call "restricted" climb: x_0 stays fixed and the dislocation can reduce its curvature only by tilting at x_0^{max}, not by further unravelling.

Restricted climb introduces a small, but finite threshold stress for the following reason. Eventually, at sufficiently small strain rates, the dislocation becomes a straight line in projection (see the calculated evolution of the dislocation profile in Fig. 6). To reach this minimum energy configuration, a small increment in line length is necessary: this is the origin of a threshold stress for climb, as has been realized before [13–15]. We neglect the possibility of "cooperative" climb as addressed by McLean [23], which is unlikely in alloys with particles of small volume fraction.

For calculating the chemical potential at AB in the case of restricted climb, the new line length increment

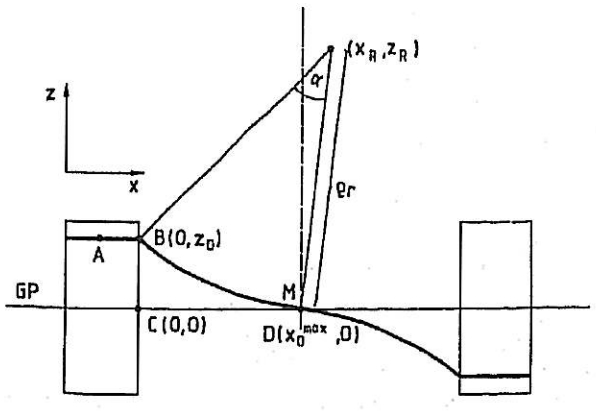

Fig. 5. Schematic profile of a dislocation after unravelling to the midpoint M between two particles, giving rise to "restricted" climb. Same projection as in Fig. 2(b).

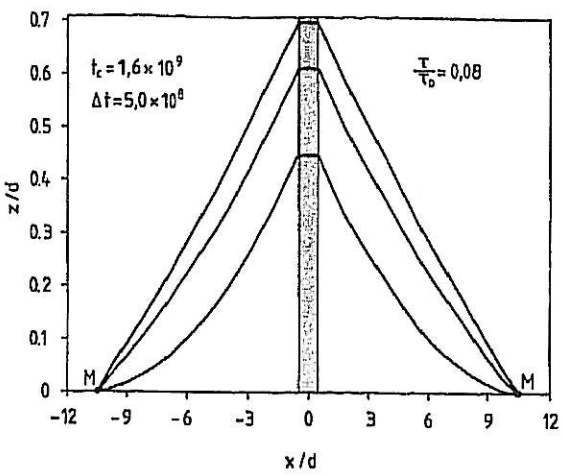

Fig. 6. Calculated dislocation profiles for $\tau = 0.08\,\tau_0$, after equidistant time steps Δt, showing climb restriction at M (same particle geometry and projection as in Fig. 4).

has to be worked out under different boundary conditions than before. The result is (see Appendix)

$$\mu_{AB}^r = \frac{2a_v}{d}\left[T_{BD}\left(\frac{x_0^{max}}{2z_r} + \frac{z_0}{x_0^{max}}\right) - \frac{\tau\lambda b}{\tan\beta}\right] \tag{13}$$

with z_r and x_0^{max} shown in Fig. 5.

At BD, the chemical potential μ_{BD}^r is given by equation (8), with

$$\rho_r = \sqrt{z_r^2 + (x_r - x_0^{max})^2} \tag{14}$$

substituted for ρ (Fig. 5, Appendix).

A dislocation normally starts in unrestricted climb and the equations of Section 3 apply. The transition to restricted climb occurs when $x_0 = x_0^{max}$. From then on, μ_{AB} [equation (6)] has to be replaced by μ_{AB}^r. By requiring $\mu_{AB}^r = \mu_{BD}^r$, the equilibrium value of z_r is determined as a function of z_0. Substituting equation (13) for μ in equation (3) yields the dislocation velocity during restricted climb.

The threshold stress is identified by setting $\mu_{AB}^r = 0$ with $z_r \to \infty$ and $z_0 = h$

$$\frac{\tau_{th}^r}{\tau_0} = \sin\left(\frac{h}{\lambda}\cdot\tan\beta\right). \tag{15}$$

This reduces to

$$\frac{\tau_{th}^r}{\tau_0} = \frac{h}{\lambda} \tag{16}$$

for small volume fractions and $\beta = \pi/4$. This expression has the same form as the "general" climb threshold obtained earlier [13, 15] for spherical particles of radius r, which amounts to $r/2\lambda$.

5. DISCUSSION OF RESULTS

The important feature of the present theoretical model is that it allows for different degrees of climb localization at the particle, depending on applied stress, and does not impose a specific shape on the

dislocation in the vicinity of the dispersoid (as in earlier models, except Lagneborg's [12] in which the kinetics however is hidden in a factor A). The unravelling distance x_0, which is a natural consequence of the equilibrium condition, increases with decreasing stress, as shown in Fig. 3. This behaviour is intuitively reasonable: because climb at the particle, unlike the unravelling process, is driven by the applied stress, climb is more localized at high stresses. Because of the simple correction for the screw component of dislocation segment BD the model becomes unstable close to the Orowan stress, therefore the maximum stress shown in Fig. 3 is $0.95\ \tau_0$. The dislocation profiles which result at a low and a high stress value are shown in Fig. 4.

The equilibrium assumption strictly rules out "local" climb: even at high stresses the value of x_0 is always greater than zero. As expected, the sharp bends necessary for "local" climb are unstable and are always relaxed to the equilibrium curvature before climb at the particle continues. It will be shown in part II [16] that a sharp bend can however be in equilibrium if an attractive particle–dislocation interaction exists.

The assumption of constant chemical potential along the climbing dislocation line is of course a simplification; it implies that, from one particle to the next, the chemical potential varies discontinuously from $+|\mu|$ to $-|\mu|$. In reality a continuous gradient will develop, subject to the appropriate Laplace equation. Taking this effect into account would however drastically complicate the formalism of the model calculations. The error introduced by our simplifying assumption is not expected to be substantial: in fact at low unravelling distances, where the exact shape of the dislocation exerts a large influence on the driving force for climb, it is negligible.

The varying degree of climb localization exerts an important influence on the creep rate in particle-

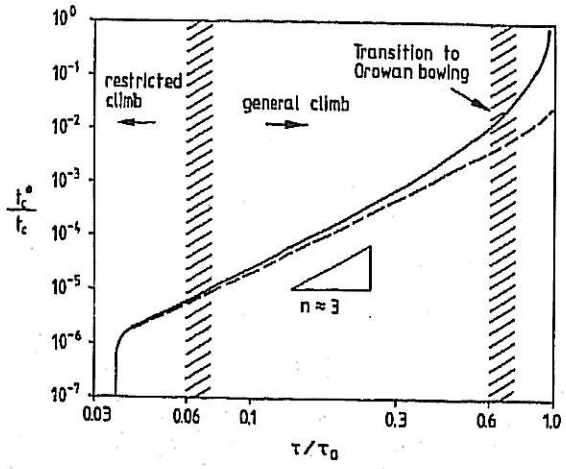

Fig. 7. Schematic illustration of dislocation velocity vs normalized stress τ/τ_0 for "non-interacting" particles. The dominant dislocation processes are identified. The dashed line gives the climb velocity neglecting particle by-passing by Orowan bowing.

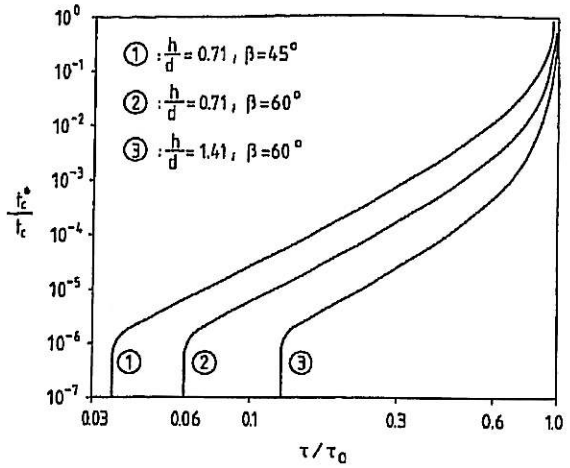

Fig. 8. Normalized dislocation velocity $(1/t_c)/(1/t_c^*)$ vs τ/τ_0 for different particle heights h and ramp angles β with $d/\lambda = 0.05$ and $1/t_c^* = 60 \cdot C_1 \cdot Gb^4 \cdot (1/d)^3$. Note that the threshold stress τ_{th}^{Γ} due to restricted climb is sensitively dependent on particle geometry whereas the slope n increases only slightly with increasing ramp angle β and aspect ratio h/d.

strengthened materials: with increasing stress fewer vacancies are required to support the equilibrium climb process, because the increment of the area under the climbing dislocation (dA_{ABD}/dy) falls rapidly as climb becomes more localized; at the same time, the dislocation curvature becomes higher when it unravels only over a short distance, and the driving force $|\mu|$ for climb [equation (8)] increases. Both effects speed up the kinetics of climb on increasing stress. Therefore the stress exponent n of the creep rate will be higher than would be expected for a dislocation with fixed climb geometry. This is illustrated in Figs 7 and 8, where the dislocation velocity (i.e. the reciprocal of the time for dislocation climb over a given particle) is plotted as a function of the normalized stress. The stress exponent varies from about $n = 3$ to 4, depending slightly on the particle parameters. It is emphasized that stress-induced diffusional processes generally lead to a linear stress dependence; the additional stress sensitivity of the creep rate is a natural consequence of the varying climb localization.

For the sake of completeness, the threshold stress due to restricted climb is also shown in Figs 7 and 8, although it is of little practical significance. Equation (15) predicts very small thresholds for low-volume fractions of particles, unless their aspect ratio h/d and ramp angle β are high. Also the present analysis gives only an upper bound, because—as has been shown in [15] and [9]—the statistics of a real particle distribution can lower this value by about an order of magnitude.

At high stresses, an essential modification has been incorporated in Figs 7 and 8. On approaching the Orowan stress, an increasing number of particles are by-passed by Orowan bowing. This effect of combined climb + Orowan bypass has been modelled in a simple way by Arzt and Ashby [15]. They argue that

in a random array the fraction of particles which are not by-passed by Orowan looping and therefore must be climbed over by the dislocations, is roughly

$$n_c = 1 - \frac{\tau}{\tau_0}. \tag{17}$$

To simulate the transition to Orowan looping, the bypass time has therefore been multiplied by n_c. The uncorrected creep rate is indicated in Fig. 7 by the dashed line.

Curves like the ones shown in Figs 7 and 8 have been calculated for several sets of particle parameters. Since these values enter the calculations in a complicated way, the results were fitted to simple expressions. They can be condensed into the following form

$$\frac{1}{t_c} = \frac{Gb^4}{d^3} \cdot C_i \cdot A \cdot \left(\frac{\tau - \tau_{th}^r}{\tau_0}\right)^n \tag{18}$$

where

$$n = 3.5\beta^{0.3}\left(\frac{h}{d}\right)^{0.2} \tag{19}$$

and

$$A = 60 \cdot 10^{-1.9\beta} \cdot \left(\frac{d}{h}\right)^{1.6} \tag{20}$$

C_i is given by equations (4) or (5), τ_{th}^r by equation (15) and τ_0 by equation (2).

Inserting for C_i and τ_0, and taking $n = 3$, the following dependences of the dislocation velocity v on the particle parameters are found

$$v \approx \frac{2\lambda}{t_c} \propto \frac{\lambda^2}{f} \propto \frac{d^2}{f^2} \tag{21}$$

for volume diffusion, and

$$v \propto \left(\frac{1}{f}\right)^{3/2} \tag{22}$$

for pipe diffusion. Hence for a given volume fraction f, the creep retardation is expected to be higher for small, closely spaced particles in the first case, and insensitive to particle size and spacing in the latter.

When predictions of the present theory are compared to measured creep data, it must be borne in mind that comparison of absolute values of creep rates are bound to remain speculative. One reason is the sensitivity of the dislocation velocity to particle geometry and distribution; to include the statistics of the climb process, a computer simulation of a dislocation climbing over an irregular array of particles with random h, d and β is presently being developed. Second, the translation of dislocation velocities into creep rates requires quantitative knowledge of the mobile dislocation density, which is usually not available.

What can be compared however is the stress sensitivity and the magnitude of the threshold stress. The model predicts stress exponents for the dislocation velocity which are not very sensitive to the particle parameters [equation (19)] and range from $n = 3$ to 4. If a stress exponent of 2, accounting for a quadratic stress dependence of dislocation density, is added, then n lies in a range which is typical of the stress dependence of the creep rate in precipitation strengthened alloys at low stresses [1–3]. That the frequently observed break in strain rate curves can be interpreted as being due to the transition from climb to particle cutting or Orowan bowing has been concluded earlier by Lagneborg and coworkers [2, 12].

By contrast, the creep behaviour of dispersion strengthened alloys cannot be explained in the framework of the present model: their threshold stresses are much too large to be identified with the threshold for restricted climb. Their stress sensitivity, which increases progressively with decreasing stress, thus cannot be rationalized on the basis of the energetics of dislocation climb over "non-interacting" particles. Hence an additional effect, such as an attractive particle–dislocation interaction, must be considered. This will be done in part II of this paper [16].

6. CONCLUSIONS

1. The kinetics of dislocation climb over hard, "non-interacting" particles has been treated without the usual arbitrary assumptions concerning dislocation shape in the vicinity of the particle. Instead, the equilibrium shape of the dislocation is calculated subject to a condition of minimum energy. The resulting dislocation velocities are expressed in approximate analytical form in equations (18)–(20).

2. The model predicts quantitatively the extent to which climb is localized near the particle. Localization increases with increasing stress but truly "local" climb is always unstable. Because fewer vacancies are required to support a more localized climb process, a natural power-law dependence of the dislocation velocity on applied stress, with $n = 3$ to 4, is obtained.

3. The predicted creep behaviour is in qualitative agreement with the behaviour of precipitation strengthened alloys, which on decreasing stress show a transition from (stress-sensitive) Orowan looping to (less stress-dependent) climb. This conclusion confirms earlier findings based on different model calculations [12].

4. The existence of a well-defined thresholds stress for creep of dispersion strengthened materials is clearly incompatible with the current model. Only a small threshold stress is predicted for equilibrium climb which is of no practical significance. Low volume fractions of small non-interacting particles are thus incapable of producing significant threshold stresses at high temperatures.

Acknowledgements—It is a pleasure to acknowledge stimulating discussions with Dr D. S. Wilkinson. Parts of this

project have been funded by the German Ministry for Research and Technology (BMFT Project Number 03M0010E4).

REFERENCES

1. R. A. Stevens and P. E. J. Flewitt, *Acta metall.* **29**, 867 (1981).
2. R. Lagneborg and B. Bergman, *Metal Sci.* **10**, 20 (1976).
3. B. Reppich, H. Bügler, R. Leistner and M. Schütze, *Creep and Fracture of Engineering Materials and Structures* (edited by B. Wilshire and D. R. J. Owen), p. 279. Pineridge Press, Swansea, U.K. (1984).
4. R. W. Lund and W. D. Nix, *Acta metall.* **24**, 469 (1976).
5. R. S. W. Shewfelt and L. M. Brown, *Phil. Mag.* **30**, 1135 (1974).
6. J. Lin and O. D. Sherby, *Res Mechanica* **2**, 151 (1981).
7. L. M. Brown, Proc. 3rd Riso Int. Symp. on Metall. Mater. Sci., Riso, p. 1 (1982).
8. R. Petkovic-Luton, D. J. Srolovitz and M. J. Luton, *Proc. Frontiers of High Temperature Mater. Conf.*, INCOMAP, London (1983).
9. W. Blum and B. Reppich, in *Creep Behaviour of Crystalline Solids* (edited by B. Wilshire and R. W. Evans), p. 83. Pineridge Press, Swansea, U.K. (1985).
10. R. F. Singer and E. Arzt, in *High Temperature Alloys for Gas Turbines and Other Applications* (edited by W. Betz, R. Brunetaud, D. Courtsouradis, H. Fischmeister, T. B. Gibbons, I. Kvernes, Y. Lindblom, J. B. Marriott and D. B. Meadowcroft), p. 97. Reidel, Dordrecht (1986).
11. L. M. Brown and R. K. Ham, in *Strengthening Methods in Crystals* (edited by A. Kelly and R. B. Nicolson), p. 9. Elsevier, Amsterdam (1971).
12. R. Lagneborg, *Scripta metall.* **7**, 605 (1973).
13. R. S. W. Shewfelt and L. M. Brown, *Phil. Mag.* **35**, 945 (1977).
14. J. H. Hausselt and W. D. Nix, *Acta metall.* **25**, 1491 (1977).
15. E. Arzt and M. F. Ashby, *Scripta metall.* **16**, 1285 (1982).
16. E. Arzt and J. Rösler, *Acta metall.* **36**, 1053 (1988).
17. M. F. Ashby, *Proc. 2nd Int. Conf. Strength of Metals and Alloys*, p. 507. Am. Soc. Metals, Metals Park, Ohio (1970).
18. V. C. Nardone and J. K. Tien, *Scripta metall.* **17**, 467 (1983).
19. D. J. Srolovitz, M. J. Luton, R. Petkovic-Luton, D. M. Barnett and W. D. Nix, *Acta metall.* **32**, 1079 (1984).
20. J. H. Schröder and E. Arzt, *Scripta metall.* **19**, 1129 (1985).
21. E. Arzt and D. S. Wilkinson, *Acta metall.* **34**, 1893 (1986).
22. J. Rösler, Doctoral Dissertation, Univ. Stuttgart (1988).
23. M. McLean, *Acta metall.* **33**, 545 (1985).

APPENDIX

Calculations

Consider an edge dislocation in a position as shown in Fig. 2. The *chemical potential* μ_{AB} *along* AB is defined as the energy change in the system when one vacancy is inserted at AB. We subtract the work done by the applied stress when the dislocation advances by dy, from the new line energy created along BD, and divide by the number of vacancies required for this advance

$$\mu_{AB} = \frac{T_{BD}\left(\frac{\partial l}{\partial y}\right)_{A_{BD}} \mathrm{d}y - \tau\lambda b\,\mathrm{d}y}{\frac{1}{a_v}\mathrm{d}A_{AB}}. \tag{A1}$$

The line length differential is evaluated with the boundary condition of constant area under the segment BD, where no vacancies are added. Taking the derivative and rearranging gives a lengthy expression which depends only on (z_0/x_0) and is well approximated by the following fit equation

$$\left(\frac{\partial l}{\partial y}\right)_{A_{BD}} \cong \tan\beta\left[1-\left(1-\frac{z_0}{x_0}\right)^{9/4}\right]. \tag{A2}$$

The increase in area under the segment AB is easily obtained for the simple particle geometry assumed in the model

$$\mathrm{d}A_{AB} = \frac{d}{2}\tan\beta\cdot\mathrm{d}y. \tag{A3}$$

By combining these equations, we get the expression for μ_{AB} given by equations (6) and (7) in the text.

The *chemical potential* μ_{BD} *along* BD is obtained similarly by expressing the infinitesimal energy change on inserting a vacancy along BD

$$\mu_{BD} = \frac{T_{BD}\left(\frac{\partial l}{\partial A_{BD}}\right)_{z_0}\mathrm{d}A_{BD}}{\frac{1}{a_v}\mathrm{d}A_{BD}}. \tag{A4}$$

Now the line length differential is evaluated for fixed z_0, because the segment AB stays in place. The area under the segment BD, projected on a plane normal to the Burgers vector, is tedious to evaluate analytically. We therefore take into account only the initial angle θ between the dislocation and the y-direction at B, for which

$$\sin\theta = \sqrt{1-(\tau/\tau_0)^2}. \tag{A5}$$

Solving for the line length differential and correcting the result for the projection effect as before, we get

$$\left(\frac{\partial l}{\partial A_{BD}}\right)_{z_0} \cong -\frac{1}{\rho}\frac{1}{\sqrt{1-(\tau/\tau_0)^2}} \tag{A6}$$

where ρ is given by equation (9) in the text. Equation (8) then results for μ_{BD}.

Next we calculate the *increment in the area* A_{ABD} under the climbing dislocation segment AD as the dislocation advances by dy, projected onto a plane perpendicular to the Burgers vector (which lies parallel to the y axis). The result is required for computing dislocation velocities according to equation (3).

We separate A_{ABD} in the following way

$$A_{ABD} = A_{AB} + A_{BD}\sqrt{1-(\tau/\tau_0)^2} \tag{A7}$$

where A_{AB} is the area under AB and A_{BD} the area under BD, with the square root factor accounting approximately for the projection, as before.

From simple geometry we get

$$A_{AB} = z_0\frac{d}{2} \tag{A8}$$

and

$$A_{BD} = \frac{x_0 z_0}{2} + \frac{x_0}{4}\left(\frac{x_0^2}{z_0}+z_0\right) - \frac{1}{8}\left(\frac{x_0^2}{z_0}+z_0\right)^2\cdot\arcsin\frac{2x_0z_0}{x_0^2+z_0^2}. \tag{A9}$$

Differentiation is now carried out as follows

$$\frac{\mathrm{d}A_{ABD}}{\mathrm{d}z_0} = \frac{\mathrm{d}A_{AB}}{\mathrm{d}z_0} + \left[\left(\frac{\partial A_{BD}}{\partial x_0}\right)_{z_0}\frac{\mathrm{d}x_0}{\mathrm{d}z_0} + \left(\frac{\partial A_{BD}}{\partial z_0}\right)_{x_0}\right]\sqrt{1-(\tau/\tau_0)^2} \tag{A10}$$

where $\mathrm{d}x_0/\mathrm{d}z_0$ is obtained from differentiating equation (10)

in the text. The result for the area differential to be inserted in equation (3) is then

$$\frac{dA_{ABD}}{dy} = \frac{dA_{ABD}}{dz_0}\tan\beta. \tag{A11}$$

The final expression is complicated but still analytical and numerical values of the dislocation velocity according to equation (3) are easily calculated with a computer.

For *restricted climb*, the radius of dislocation curvature is ρ_r as given by equation (14) in the text (see also Fig. 5). ρ_r must be substituted for ρ in equation (8) to give μ^r_{BD}. To obtain the chemical potential along AB, the line length differential in equation (A1) must be evaluated subject to the condition that x_0 is fixed. Taking the appropriate derivatives again leads to an extremely complicated expressions for which the following fit equation has been obtained

$$\left(\frac{\partial l}{\partial y}\right)^r_{A_{BD}} \cong \left(\frac{x_0^{max}}{2z_r} + \frac{z}{x_0^{max}}\right)\tan\beta. \tag{A12}$$

The resulting approximate expression for μ^r_{AB} is given in equation (13) in the text. The area increment dA_{ABD}/dy is calculated for the new boundary conditions and incorporated in the numerical evaluation of equation (3).